

AD-A066 608

R AND D ASSOCIATES MARINA DEL REY CALIF
ON THE IONOSPHERIC PARAMETERS WHICH GOVERN HIGH LATITUDE ELF PR--ETC(U)
SEP 78 C GREIFINGER, P GREIFINGER

F/G 20/14

DNA001-78-C-0009

UNCLASSIFIED

RDA-TR-107005-004

DNA-4685T

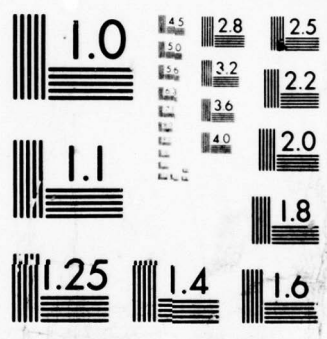
NL

| OF |
AD
A066608



END
DATE
FILMED

'5--79'
DDC



MICROCOPY RESOLUTION TEST CHART
NATIONAL BUREAU OF STANDARDS-1963-A

✓

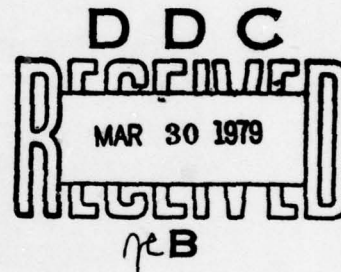
① LEVEL

DNA 4685T

AD A0 66608

ON THE IONOSPHERIC PARAMETERS WHICH GOVERN HIGH LATITUDE ELF PROPAGATION IN THE EARTH-IONOSPHERE WAVEGUIDE

Carl Greifinger
Phyllis Greifinger
R & D Associates
P. O. Box 9695
Marina del Rey, California 90291



30 September 1978

Topical Report for Period 16 October 1977—30 September 1978

CONTRACT No. DNA 001-78-C-0009

APPROVED FOR PUBLIC RELEASE;
DISTRIBUTION UNLIMITED.

THIS REPORT SPONSORED BY THE DEFENSE NUCLEAR AGENCY
UNDER RDT&E RMSS CODE B310078464 P99QAXDB00136 H2590D.

Prepared for
Director
DEFENSE NUCLEAR AGENCY
Washington, D. C. 20305

DDC FILE COPY

79 02 01 044

Destroy this report when it is no longer
needed. Do not return to sender.

PLEASE NOTIFY THE DEFENSE NUCLEAR AGENCY,
ATTN: TISI, WASHINGTON, D.C. 20305, IF
YOUR ADDRESS IS INCORRECT, IF YOU WISH TO
BE DELETED FROM THE DISTRIBUTION LIST, OR
IF THE ADDRESSEE IS NO LONGER EMPLOYED BY
YOUR ORGANIZATION.



UNCLASSIFIED

SECURITY CLASSIFICATION OF THIS PAGE (When Data Entered)

19 REPORT DOCUMENTATION PAGE		READ INSTRUCTIONS BEFORE COMPLETING FORM	
1. REPORT NUMBER DNA 4685T	2. GOVT ACCESSION NO.	3. RECIPIENT'S CATALOG NUMBER	
4. TITLE (and Subtitle) ON THE IONOSPHERIC PARAMETERS WHICH GOVERN HIGH LATITUDE ELF PROPAGATION IN THE EARTH- IONOSPHERE WAVEGUIDE.		5. TYPE OF REPORT & PERIOD COVERED Topical Report, for Period 16 Oct 77-30 Sep 78	
7. AUTHOR(s) Carl Greifinger Phyllis Greifinger		6. PERFORMING ORG. REPORT NUMBER RDA-TR-107005-004	
9. PERFORMING ORGANIZATION NAME AND ADDRESS R&D Associates P.O. Box 9695 Marina del Rey, California 90291		8. CONTRACT OR GRANT NUMBER(s) DNA 001-78-C-0009	
11. CONTROLLING OFFICE NAME AND ADDRESS Director Defense Nuclear Agency Washington, D.C. 20305		10. PROGRAM ELEMENT, PROJECT, TASK AREA & WORK UNIT NUMBERS Subtask P99QAXDB001-36	
14. MONITORING AGENCY NAME & ADDRESS (if different from Controlling Office) B001		12. REPORT DATE 30 Sep 1978	
		13. NUMBER OF PAGES 32	
		15. SECURITY CLASS (of this report) UNCLASSIFIED	
		15a. DECLASSIFICATION/DOWNGRADING SCHEDULE	
16. DISTRIBUTION STATEMENT (of this Report) Approved for public release; distribution unlimited.			
17. DISTRIBUTION STATEMENT (of the abstract entered in Block 20, if different from Report)			
18. SUPPLEMENTARY NOTES This work sponsored by the Defense Nuclear Agency under RDT&E RMSS Code B310078464 P99QAXDB00136 H2590D.			
19. KEY WORDS (Continue on reverse side if necessary and identify by block number) Radio Propagation ELF High Latitude			
20. ABSTRACT (Continue on reverse side if necessary and identify by block number) An approximate wave solution is obtained for the propagating ELF mode at high latitudes in the Earth-ionosphere waveguide. A simple approximate expression for the complex propagation constant emerges from the solution. The propa- gation constant depends on four parameters, two altitudes and a scale height associated with each altitude. The lower altitude is the height at which the conduction current parallel to the magnetic field becomes equal to the dis- placement current. The associated scale height is the local scale height of			

DD FORM 1 JAN 73 1473 EDITION OF 1 NOV 65 IS OBSOLETE

UNCLASSIFIED

SECURITY CLASSIFICATION OF THIS PAGE (When Data Entered)

390 124 79 02 01 044

UNCLASSIFIED

SECURITY CLASSIFICATION OF THIS PAGE(When Data Entered)

20. ABSTRACT (Continued)

the parallel conductivity. Under daytime ionospheric conditions, the upper altitude is the height at which the local wave number becomes equal to the reciprocal of the local scale height of the refractive index. The associated scale height is the local scale height of the refractive index. Under the simplest nighttime conditions, the second set of parameters is replaced by the altitude of the E-region bottom and the local wave number just inside the E-region. The relative phase velocity depends, in first approximation, only on the ratio of the two altitudes. The attenuation rate depends on the other two parameters, as well. The two principal attenuation mechanisms are Joule heating by longitudinal currents in the vicinity of the lower altitude and energy leakage of the whistler component of the ELF wave at the upper altitude.

UNCLASSIFIED

SECURITY CLASSIFICATION OF THIS PAGE(When Data Entered)

PREFACE

The authors are indebted to Dr. William F. Moler of Naval Ocean Systems Center for providing full-wave calculations for comparison with our approximate results.

ACCESSION for		
NTIS	White Section	<input checked="" type="checkbox"/>
DDC	Buff Section	<input type="checkbox"/>
UNANNOUNCED		<input type="checkbox"/>
JUSTIFICATION _____		
BY _____		
DISTRIBUTION/AVAILABILITY CODES		
Dist. AVAIL and/or SPECIAL		
A		

TABLE OF CONTENTS

<u>Section</u>	<u>Page</u>
1. INTRODUCTION.	3
2. BASIC EQUATIONS	6
3. APPROXIMATE SOLUTIONS AND EIGENVALUES	9
3.1 Vacuum and Lower Ionosphere.	9
3.2 Middle and Upper Ionosphere.	10
3.2.1 Daytime Ionospheric Conditions.	12
3.2.2 Nighttime Ionospheric Conditions.	17
4. NUMERICAL RESULTS AND CONCLUSIONS	20
BIBLIOGRAPHY.	25

SECTION 1. INTRODUCTION

In a recent paper (Greifinger and Greifinger [1978], hereinafter referred to as I), the authors derived an approximate expression for the complex propagation constant for ELF propagation in the Earth-ionosphere waveguide. The theory was developed for an ionosphere that was sufficiently disturbed that there was no significant penetration of the electromagnetic field to altitudes where anisotropy due to the Earth's magnetic field had to be taken into account. It was shown that the propagation constant is determined by four parameters, two frequency-dependent altitudes and the local conductivity scale heights at those altitudes. The lower altitude, denoted by h_o , is where the conduction current becomes equal to the displacement current, and the higher altitude, denoted by h_1 , is where the local reciprocal wave number becomes equal to the local scale height of the refractive index. There is a Joule heating maximum at h_o arising from predominantly vertical currents, and a secondary maximum in the vicinity of h_1 arising from predominantly horizontal currents. At altitudes in the vicinity of and below h_o , the electric field is predominantly vertical, and energy flow in the waveguide is in the horizontal direction. Within a few scale heights above h_o , the electric field becomes horizontally polarized, and energy flow is vertical.

In this paper, the theory developed in I is extended to include the effects of anisotropy. For the sake of mathematical simplicity, it is assumed that the Earth's field is vertical, which limits the validity of the theory, strictly speaking, to high magnetic latitudes. The generalization to arbitrary dip angle is straightforward, though somewhat tedious. It turns out, however, that there is no significant dependence of the propagation constant on magnetic latitude except very

close to the magnetic equator, so the results have a rather large geographic range of applicability.

When anisotropy is included, the parameters which determine the propagation constant differ for daytime and nighttime ionospheric conditions. In both cases, two parameters which enter are the frequency-dependent altitude h_o at which the conduction current parallel to the magnetic field becomes equal to the displacement current, and the local scale height of the parallel conductivity σ_o . Under daytime conditions, two additional pairs of altitudes (frequency-dependent) and scale heights appear as parameters. One pair is the altitude at which the local reciprocal wave number for vertically propagating O waves becomes equal to the local scale height of the refractive index, and the scale height of this refractive index. The other pair are the corresponding quantities for vertically propagating X (whistler) waves. It is assumed in this paper that these altitudes are attained in a region of the ionosphere where $|\sigma_H| \gg |\sigma_p|$, σ_H being the Hall conductivity and σ_p the Pedersen conductivity. Under these conditions, which apply over a substantial altitude range, the two pairs of parameters become identical and the analysis is somewhat simpler. The vicinity of the single altitude h_1 is in this case a region of reflection, rather than of significant heating, as was the case for the isotropic ionosphere. The O wave undergoes nearly total reflection at this altitude, but some of the X wave energy leaks out of the waveguide, thereby contributing to the attenuation.

For typical nighttime conditions, a sharp reflecting E-region bottom may be encountered before the local reciprocal wave number becomes equal to the local scale height. Under such circumstances, the altitude of the E-region bottom replaces

h_1 as a parameter, and the refractive index scale height is replaced by the local wavelength on the E-region side of the bottom.

As in I, the approximate propagation constants are given by simple algebraic expressions involving the various parameters. Numerical results have been obtained for a hypothetical daytime ionospheric profile in which the electron density is assumed to increase exponentially with altitude and the electron collision frequency to decrease exponentially with altitude. The results are in excellent agreement with full-wave calculations for the same profile which were carried out by Dr. William Moler of Naval Ocean Systems Center. The agreement lends support to the physical assumptions on which the theory is based.

Booker and Lefeuvre (1977) have also proposed a method for the calculation of approximate ELF propagation constants in the anisotropic Earth-ionosphere waveguide. The method is based on a simplified model of the waveguide in which the ionosphere is cut off discontinuously at a frequency-dependent level and abolished below this level. The altitude at which the ionosphere is truncated corresponds very closely to the altitude h_1 , and their treatment of the fields above this level is quite similar to ours. In their formulation, the region around h_o , which plays a unique and important role in our theory, is treated as part of the vacuum. This results in a predicted phase velocity which is in general significantly higher than that obtained from our theory. They attempt to account for the attenuation due to Joule heating at levels below their truncated ionosphere, but do so in a manner which may seriously overestimate the size of the effect, especially at the low end of the ELF band.

SECTION 2. BASIC EQUATIONS

It will be assumed that the Earth-ionosphere waveguide is horizontally stratified and, as discussed in the Introduction, that the geomagnetic field is in the vertical (z) direction. The equations governing electromagnetic propagation in the anisotropic waveguide are, of course, Maxwell's equations

$$\vec{\nabla} \times \vec{E} = i\omega\vec{B} \quad (1)$$

$$\vec{\nabla} \times \vec{B} = \mu_0 \vec{j} - i\frac{\omega}{c^2} \vec{E}, \quad (2)$$

where we have assumed a time dependence $e^{-i\omega t}$, and the generalized Ohm's law

$$\vec{j} = \sigma_0 (\vec{E} \cdot \hat{e}_z) \hat{e}_z + \sigma_p [\vec{E} - (\vec{E} \cdot \hat{e}_z) \hat{e}_z] + \sigma_H (\vec{E} \times \hat{e}_z), \quad (3)$$

where \hat{e}_z is a unit vector in the z direction and σ_0 , σ_p , and σ_H are the parallel, Pedersen, and Hall conductivities, respectively. The fields can be written in terms of the customary potentials as

$$\vec{B} = \vec{\nabla} \times \vec{A} \quad (4)$$

$$\vec{E} = \vec{\nabla}\psi + i\omega\vec{A}. \quad (5)$$

Combining Eq. (4) with the time derivative of Eq. (2), we obtain

$$i\omega[\vec{\nabla}(\vec{\nabla} \cdot \vec{A}) - \nabla^2 \vec{A}] - i\mu_0 \omega \vec{j} - k^2 \vec{E} = 0. \quad (6)$$

The modal solutions of this equation are obtained by a separation of variables. The rectangular components of \vec{A} and the potential ψ satisfy a two-dimensional wave equation

$$(\nabla_1^2 + k^2 S^2)F = 0, \quad (7)$$

where ∇_1^2 is the Laplacian operator in the horizontal plane and kS is the (complex) horizontal propagation constant for the mode.

At ELF, only the lowest mode is non-evanescent in the Earth-ionosphere waveguide. In the absence of anisotropy, this is a TM mode which is derivable from a vector potential with only a vertical component A_z . When anisotropy is included, the lowest mode acquires a TE component, which requires a horizontal component of the vector potential. It will be shown that all the boundary conditions can be satisfied by a vector potential of the form

$$\vec{A} = A_z \hat{e}_z - \frac{1}{(i\omega)} \vec{\nabla} \times (u \hat{e}_z), \quad (8)$$

where u is a scalar function.

The various relations above may now be incorporated into Eq. (6) to obtain a set of coupled equations for the system. The vertical component of Eq. (6) becomes

$$\frac{\partial \psi}{\partial z} = -i\omega A_z \left[1 - \frac{S^2}{\left(1 + \frac{i\sigma_0}{\epsilon_0 \omega} \right)} \right], \quad (9)$$

while the horizontal component becomes

$$\begin{aligned}
& (\hat{e}_z \times \vec{\nabla}) [\nabla^2 u + (i\mu_0 \omega \sigma_p + k^2)u - i\mu_0 \omega \sigma_H \psi] \\
& - \vec{\nabla}_1 [i\omega \vec{\nabla} \cdot \vec{A} - (i\mu_0 \omega \sigma_p + k^2)\psi - i\mu_0 \omega \sigma_H u] = 0 .
\end{aligned}
\tag{10}$$

A gauge condition remains to be specified. A convenient choice is clearly

$$i\omega \vec{\nabla} \cdot \vec{A} = (i\mu_0 \omega \sigma_p + k^2)\psi + i\mu_0 \omega \sigma_H u , \tag{11}$$

which removes the terms involving $\vec{\nabla}_1$ from Eq. (10). The contents of the first brackets must then also vanish, which gives

$$\frac{\partial^2 u}{\partial z^2} = -[i\mu_0 \omega \sigma_p + k^2(1 - S^2)]u + i\mu_0 \omega \sigma_H \psi . \tag{12}$$

The basic equations are (9), (11), and (12), in which S appears as an eigenvalue parameter. The eigenvalue is determined by solving these coupled equations with appropriate boundary conditions at the ground and at large altitudes. An approximate method for determining the eigenvalue, similar to that developed in I, will be presented below. The method consists of constructing two approximate analytic solutions of the equations. One solution obeys the proper boundary conditions at the ground and is valid up to an altitude a few scale heights above h_0 . The other obeys the proper boundary conditions at large altitudes and is valid down to an altitude a few scale heights below h_1 . There is a common altitude region where both solutions are valid. The eigenvalue is determined by requiring that the leading terms of the two solutions agree in the overlap region.

SECTION 3. APPROXIMATE SOLUTIONS AND EIGENVALUES

3.1 VACUUM AND LOWER IONOSPHERE

The conductivities of the medium are increasing functions of altitude. As in I, we define a frequency-dependent altitude h_0 at which the parallel conduction current becomes equal to the displacement current. Between the ground and a few conductivity scale heights above h_0 , the right-hand sides of Eq. (11) and (12) are very small, and these equations become approximately

$$\frac{\partial A_z}{\partial z} = 0 \quad (13)$$

$$\frac{\partial^2 u}{\partial z^2} = 0 \quad (14)$$

At ELF, the ground may be considered as perfectly conducting, and the appropriate boundary condition is therefore $E_{x,y}(0) = 0$. This in turn requires $\psi(0) = u(0) = 0$. The solution of Eqs. (9), (13), and (14) satisfying these boundary conditions is

$$A_z = A_0 \quad (\text{constant}) \quad (15)$$

$$u = \beta z \quad (16)$$

$$\psi = -i\omega A_0 \left[z - s^2 \int_0^z \frac{dz}{\left(1 + \frac{i\sigma_0}{\epsilon_0 \omega}\right)} \right] \quad (17)$$

The integrand in Eq. (17) is essentially unity up to a conductivity scale height or so below h_0 and becomes very small a few scale heights above this altitude. It is therefore necessary to represent σ_0 accurately only in the neighborhood of h_0 , where a simple exponential provides a very good approximation. Thus, we write

$$\sigma_0 = \epsilon_0 \omega e^{(z-h_0)/\zeta_0}, \quad (18)$$

where ζ_0 is the local scale height at h_0 . The integral in Eq. (17) can now be evaluated, giving

$$\psi = -i\omega A_0 \left\{ z - S^2 \left[h_0 - \frac{i\pi}{2}\zeta_0 - \zeta_0 \ln \left(1 - ie^{(h_0-z)/\zeta_0} \right) \right] \right\} \quad (19)$$

The constant β and the eigenvalue S remain to be determined.

3.2 MIDDLE AND UPPER IONOSPHERE

A few scale heights above h_0 , the parallel current becomes much larger than the displacement current, and Eq. (9) becomes approximately

$$\frac{\partial \psi}{\partial z} + i\omega A_z = 0 \quad (20)$$

The left-hand side of Eq. (20) is exactly the vertical component of the electric field, which thus becomes very small somewhat above h_0 . The electric field thus undergoes an important transition from vertical to horizontal polarization in the region around h_0 .

At the altitudes in question, the Pedersen and Hall currents are also much larger than the displacement current, so that the terms proportional to k^2 in Eqs. (11) and (12) may be neglected (a QL approximation). These equations therefore become

$$\frac{\partial^2 \psi}{\partial z^2} + i\mu_0 \omega \sigma_p \psi + i\mu_0 \omega \sigma_H u = 0 \quad (21)$$

$$\frac{\partial^2 u}{\partial z^2} + i\mu_0 \omega \sigma_p u - i\mu_0 \omega \sigma_H \psi = 0 , \quad (22)$$

where A_z has been eliminated by use of Eq. (20).

If we introduce as variables

$$\psi_{\pm} = \psi \pm iu , \quad (23)$$

we obtain the two uncoupled wave equations

$$\frac{\partial^2 \psi_{\pm}}{\partial z^2} + n_{\pm}^2 k^2 \psi_{\pm} = 0 \quad (24)$$

where

$$n_{\pm}^2 = \frac{1}{\epsilon_0 \omega} (i\sigma_p \pm \sigma_H) . \quad (25)$$

The upper sign corresponds to vertical O wave propagation and the lower sign to vertical X wave (whistler) propagation. These equations must be solved subject to the radiation boundary condition at large altitudes.

3.2.1 Daytime Ionospheric Conditions

Following the procedure of I, we will construct an approximate solution of the upper ionosphere equations which satisfies the boundary condition at large altitudes and which has a common region of validity with the lower ionosphere solution. This involves the introduction of the altitude h_1 , at which the local wave number $|n|k$ is equal to the reciprocal of the refractive index scale height. Under highly disturbed daytime conditions, this occurs at an altitude where the ionosphere is nearly isotropic, i.e., where

$$n_+^2 \cong n_-^2 = \frac{i\sigma}{\epsilon_0 \omega} \quad (26)$$

This was the case treated in I, for which the eigenvalue was shown to be

$$s^2 = \frac{(h_1 + i\frac{\pi}{2}\zeta_1)}{(h_0 - i\frac{\pi}{2}\zeta_0)}, \quad (27)$$

where ζ_1 is the conductivity scale height at the altitude h_1 . The altitudes h_0 and h_1 were shown to be locations of maximum Joule heating, the lower altitude maximum being associated with vertical currents and the higher altitude maximum with horizontal currents. There was no significant field penetration much above the altitude h_1 .

Under normal daytime conditions, and over most of the ELF band, the altitude h_1 occurs where $|\sigma_H| \gg |\sigma_P|$, i.e., where

$$n_+^2 \cong -n_-^2 \cong \frac{\sigma_H}{\epsilon_0 \omega} = -n^2 \quad (28)$$

In the vicinity of h_1 , we may approximate the index of refraction by an exponential with a scale height appropriate to that altitude. Thus we write

$$n^2 = n_1^2 e^{(z-h_1)/\zeta_1} \quad (29)$$

where h_1 is defined as the frequency-dependent altitude at which

$$2|n_1|k\zeta_1 = 1. \quad (30)$$

(The scale height for the refractive index has been taken as $2\zeta_1$ for consistency with the theory for the isotropic ionosphere.)

Since the imaginary part of σ_H is very small, the quantity n_1 is nearly real. The outgoing wave solutions of Eq. (24) are then

$$\psi_+ = aH_O^{(1)}(iy) \quad (31)$$

$$\psi_- = \gamma aH_O^{(1)}(y) \quad (32)$$

$$y = e^{(z-h_1)/2\zeta_1} \quad (33)$$

where a and γ are constants to be determined. The potential functions ψ and u , as determined from Eq. (23), are

$$\psi = \frac{a}{2} \left[H_O^{(1)}(iy) + \gamma H_O^{(1)}(y) \right] \quad (34)$$

$$u = \frac{a}{2i} \left[H_O^{(1)}(iy) - \gamma H_O^{(1)}(y) \right]. \quad (35)$$

The potentials given by Eqs. (34) and (35) must agree with Eqs. (16) and (19), respectively, in the altitude range $h_0 \ll z \ll h_1$, where both approximations are valid. In this altitude range, $|y| \ll 1$ and the Hankel functions may be approximated by their small argument expansions. The leading terms give

$$u \rightarrow \frac{a}{2\pi\zeta_1} \left[(1 + \gamma)(z - h_1) + i\pi\gamma\zeta_1 \right] \quad (36a)$$

$$\psi \rightarrow \frac{ia}{2\pi\zeta_1} \left[(1 - \gamma)(z - h_1) - i\pi\gamma\zeta_1 \right]$$

$$(h_0 \ll z \ll h_1) . \quad (36b)$$

Matching these functions to the leading terms of the lower ionosphere solutions in the same altitude range, we obtain

$$\gamma = \frac{h_1}{(h_1 + i\pi\zeta_1)} \quad (37)$$

$$s^2 = \frac{h_1(h_1 + i\pi\zeta_1)}{(h_0 - i\frac{\pi}{2}\zeta_0)(h_1 + \frac{i\pi}{2}\zeta_1)} . \quad (38)$$

Although this completes the derivation of the approximate eigenvalue, there are two additional relationships which exist among the three remaining undetermined constants. These are

$$\frac{a}{A_0} = -2\pi\omega \frac{\zeta_1(h_1 + i\pi\zeta_1)}{(2h_1 + i\pi\zeta_1)} \quad (39)$$

$$\frac{\beta}{A_0} = -i\pi\omega \frac{\zeta_1}{(2h_1 + i\pi\zeta_1)} , \quad (40)$$

with A_0 remaining as an arbitrary normalization factor. An approximate analytic solution has thus been obtained not only for the eigenvalue, but for the height dependence of the various field components as well.

The approximate eigenvalue given by Eq. (38) is slightly different from its counterpart for the isotropic ionosphere given by Eq. (27). However, since $\zeta_0/h_0 \ll 1$ and $\zeta_1/h_1 \ll 1$, both eigenvalues are to first approximation

$$s \approx \left(\frac{h_1}{h_0}\right)^{\frac{1}{2}} \left[1 + \frac{i\pi}{4} \left(\frac{\zeta_0}{h_0} + \frac{\zeta_1}{h_1} \right) \right] . \quad (41)$$

The relative phase velocity is thus approximately

$$\frac{v}{c} \approx \left(\frac{h_0}{h_1}\right)^{\frac{1}{2}} , \quad (42)$$

and the horizontal attenuation rate in decibels per megameter is approximately

$$\alpha \approx .143 f \left(\frac{h_1}{h_0}\right)^{\frac{1}{2}} \left(\frac{\zeta_0}{h_0} + \frac{\zeta_1}{h_1} \right) , \quad (43)$$

where f is the frequency in Hertz. Thus, in first approximation, the relative phase velocity depends only on the ratio of the two altitudes, and is independent of the scale heights. This is quite different from the theory of Booker and Lefeuvre

(1977), in which the relative phase velocity differs from unity by an amount proportional to ζ_1/h_1 .

The horizontal attenuation in the waveguide arises from two sources. The part proportional to ζ_0/h_0 is due to Joule heating by vertical currents, which has a maximum at h_0 as in the isotropic case. However, the part proportional to ζ_1/h_1 is no longer associated with Joule heating by horizontal currents. The horizontal currents are now Hall currents, which are non-dissipative. The field at this altitude has been decomposed by the anisotropic medium into two vertically propagating waves, an O wave component whose index of refraction is almost purely imaginary and an X wave component whose index is almost purely real. Thus, the O wave undergoes total reflection in this region, whereas some of the X wave energy leaks out of the waveguide. The part of the attenuation rate proportional to ζ_1/h_1 is associated with this leakage, as pointed out by Booker and Lefeuvre (1977), who obtained a very similar result for this quantity. The reflected part of the X wave results in a small TE component in the field at the ground. From Eqs. (4), (8), (16), and (40), the ratio of the TE and TM components at the ground is

$$\frac{B_{TE}}{B_{TM}} = \left(-\frac{1}{i\omega A_z} \frac{\partial u}{\partial z} \right)_{z=0} = -\frac{\beta}{i\omega A_0} = \frac{\pi \zeta_1}{(2h_1 + i\pi \zeta_1)} \quad (44)$$

The magnetic field at the ground thus has slight elliptical polarization, with the major axis nearly perpendicular to the plane of propagation.

The theory has been developed under the assumption that h_1 is reached at an altitude where $|\sigma_H| \gg |\sigma_p|$. If the criterion is met where the Pedersen conductivity is not negligible, there

is a separate pair of values of h_1 and ζ_1 for the O and the X components, which in general differ only slightly. It is not difficult to generalize the theory to this situation. This results, however, in only a small correction to the eigenvalue obtained by replacing the two pairs of parameters by their average.

3.2.2 Nighttime Ionospheric Conditions

Under nighttime conditions, a sharp E-region bottom is usually encountered before the altitude h_1 is established. The electron density undergoes a very sharp increase in passing through the bottom, above which it can be quite variable. We will consider only the simplest model where the density above this bottom varies slowly on the scale of the local wavelength. Under such conditions, the phase integral approximation is valid above the E-region bottom, and we may take as solutions of Eq. (24)

$$\psi_{\pm} = \Lambda_{\pm} (n_{\pm} k)^{-\frac{1}{2}} \exp \left\{ i k \int_{h_E}^z n_{\pm}(z) dz \right\} \quad (45)$$

where h_E is the altitude of the E-region bottom and Λ_{\pm} are constants. The associated potential functions ψ and u have the form

$$\psi = \Lambda (\psi_- + \delta \psi_+) \quad (46)$$

$$u = i \Lambda (\psi_- - \delta \psi_+) \quad (47)$$

where Λ and δ are constants to be determined. Under nighttime conditions, the solution up to the E-region bottom is well

approximated by Eqs. (16) and (19). The boundary conditions require that the tangential electric and magnetic fields be continuous at $z = h_E$. This, in turn, requires the continuity of u , $\frac{du}{dz}$, ψ , and $\frac{d\psi}{dz}$ at this interface. If we assume, as in Eq. (28), that

$$n_+^2(h_E) \cong n_-^2(h_E) \cong -n_E^2, \quad (48)$$

then application of the boundary conditions leads to

$$s^2 = \frac{h_E}{(h_0 - i\frac{\pi}{2}\zeta_0)} \left\{ 1 + \frac{\epsilon}{2} \left[\frac{1 + i(1+2\epsilon)}{1 + \frac{1}{2}\epsilon(1+i)} \right] \right\} \quad (49)$$

where

$$\epsilon = \frac{1}{kn_E h_E}. \quad (50)$$

Assuming that n_E is nearly real, the eigenvalue is in first approximation

$$s \approx \left(\frac{h_E}{h_0} \right)^{\frac{1}{2}} \left[1 + i \left(\frac{\pi}{4} \frac{\zeta_0}{h_0} + \frac{1}{4kn_E h_E} \right) \right] \quad (51)$$

Comparison with the daytime results shows that the altitude of the E-region bottom has replaced the frequency-dependent altitude h_1 as a parameter and the local wavelength just inside the E-region has replaced ζ_1 . The physical processes occurring at h_E are the same as those associated with h_1 , namely nearly total reflection of the O wave and partial leakage of the X wave. Although we have considered only the simplest case of a

single reflecting boundary, the method can obviously be generalized to include any number of such discontinuities.

SECTION 4. NUMERICAL RESULTS AND CONCLUSIONS

The validity of the theory has been examined by comparing approximate eigenvalues with a full-wave calculation for a hypothetical daytime conductivity profile. For simplicity, it was assumed that only electrons contributed to the conductivity at all altitudes. Although this assumption may be unrealistic, it does not invalidate a comparison of an approximate solution with a full-wave solution for the same profile. The electron density and collision frequency profiles were assumed to be simple exponentials

$$N_e = N_0 e^{z/\zeta_e} \quad (52)$$

$$\nu = \nu_0 e^{-z/\zeta_\nu} \quad (53)$$

with $N_0 = 3.73 \times 10^3/\text{m}^3$, $\nu_0 = 1.63 \times 10^{12} \text{sec}^{-1}$, and $\zeta_e = \zeta_\nu = 6 \text{ km}$. With these profiles, the conductivities

$$\sigma_o = \epsilon_o \frac{\omega_p^2}{(\nu_e - i\omega)} \quad (54)$$

$$\sigma_p = \epsilon_o \frac{\omega_p^2 (\nu_e - i\omega)}{(\nu_e - i\omega)^2 + \omega_e^2} \quad (55)$$

$$\sigma_H = -\epsilon_o \frac{\omega_p^2 \omega_e}{(\nu_e - i\omega)^2 + \omega_e^2} \quad (56)$$

were calculated, taking $\omega_e = 10^7 \text{ rad/sec}$ as the electron gyro-frequency. From the calculated conductivity profiles, the parameters h_o , ζ_o , h_1 , and ζ_1 were determined for

frequencies of 50 Hertz and 100 Hertz, and the approximate eigenvalues were calculated from Eq. (38). A full-wave calculation for the profiles given by Eqs. (52) and (53) was carried out by Dr. William Moler of Naval Ocean Systems Center for comparison with the approximate eigenvalues. The two sets of results are shown in Table 1. The phase speeds agree to better than 1% and the attenuation rates to within 0.2 decibels per megameter, which is quite good.

The relative phase speeds predicted by the theory of Booker and Lefeuvre for the same profile are approximately 0.95 at both frequencies, which is substantially higher than the full-wave values. We have not attempted to calculate their attenuation rates, which requires integration over the conductivity profile to estimate the contribution from Joule heating below h_1 . However, an important assumption on which their approximation is based is clearly at variance with our analysis. They calculate the fraction of energy removed from the horizontal flow by Joule heating at a given altitude, and identify the attenuation rate with the average value of this quantity between the ground and h_1 . This identification relies on the assumption that the horizontal flow of energy is approximately uniform between the surface of the earth and the level of reflection. However, the lower ionosphere solutions presented here show that, while the horizontal magnetic field remains essentially constant in this region, the vertical electric field falls off quite rapidly above h_0 . To lowest order in ζ_0/h_0 , the rate of horizontal flow of energy is

$$\text{Re}(E_z B_1^*) = \frac{\omega^2}{\mu_0 c} \frac{\text{Re}(S) |S|^2 |A_0|^2}{\left[1 + \left(\frac{\sigma_0}{\epsilon_0 \omega} \right)^2 \right]} \quad (57)$$

Table 1. Comparison of Approximate- and Full-Wave Propagation Constants for the Hypothetical Daytime Ionosphere Described in Section 4.

f (Hz)	IONOSPHERIC PARAMETERS				APPROXIMATE		FULL - WAVE	
	h_o (km)	z_o (km)	h_1 (km)	z_1 (km)	v/c	dB/1000 km	v/c	dB/1000 km
50	52.7	3	86	6	.78	1.1	.78	1.2
100	55	3	82	5.8	.82	2.2	.82	2.0

4
where we have assumed σ_0 to be real. For an exponential conductivity profile, the horizontal flow rate is essentially constant to an altitude h_0 , above which it falls off rapidly. The Joule heating rate is given by

$$\sigma_0 |E_z|^2 = \frac{\omega^2 |S|^4 |A_0|^2 \sigma_0}{\left[1 + \left(\frac{\sigma_0}{\epsilon_0 \omega} \right)^2 \right]}, \quad (58)$$

which exhibits a very sharp maximum at h_0 , and becomes very small within a scale height or so on either side of this altitude. (These points are illustrated graphically in I.) For the profile given by Eq. (18), the heating and flow rates can be integrated over altitude analytically. Since the integrands fall off very rapidly above h_0 , little error is made by extending the upper limit to infinity. The result is

$$\frac{\int_0^\infty \sigma_0 |E_z|^2 dz}{\int_0^\infty \text{Re}(E_z B_1^*) dz} = k \frac{\pi}{2} \frac{\zeta_0}{h_0} \text{Re}(S), \quad (59)$$

which agrees exactly with the horizontal attenuation rate due to heating as calculated from Eq. (41).

Although essentially all of the heating dissipation takes place in a narrow altitude region around h_0 , the local attenuation rate (i.e., the ratio of the local heating rate to the horizontal flow rate at the same level) is an increasing function of altitude. Thus, an unweighted average of the local attenuation rate will exceed the actual horizontal attenuation rate. For a given profile, the difference

between the two values increases with decreasing frequency due to the lowering of the altitude h_0 . This perhaps accounts for the difficulty experienced by Booker and Lefeuvre (1978) in reconciling the observability of the nighttime Schumann resonance with generally accepted nighttime profiles.

BIBLIOGRAPHY

- Booker, H. G., and F. Lefeuvre, "The Relation Between Ionospheric Profiles and ELF Propagation in the Earth-Ionosphere Transition Line," J. Atmos. Terr. Phys., Vol. 39, pp. 1277-1292, 1977.
- Greifinger, C., and P. Greifinger, "Approximate Method for Determining ELF Eigenvalues in the Earth-Ionosphere Waveguide," Rad. Sci., 1978 (to be published).

DISTRIBUTION LIST

DEPARTMENT OF DEFENSE

Assistant Secretary of Defense
Comm, Cmd, Cont. & Intell.
ATTN: M. Epstein
ATTN: J. Babcock

Assistant to the Secretary of Defense
Atomic Energy
ATTN: Executive Assistant

Command & Control Technical Center
Department of Defense
ATTN: C-650, G. Jones

Defense Advanced Rsch. Proj. Agency
ATTN: TIO

Defense Communication Engineer Center
ATTN: Code 720, J. Worhtington
ATTN: Code R410, J. McLean

Defense Communications Agency
ATTN: Code 101B
ATTN: Code R1033, M. Raffensperger

Defense Documentation Center
12 cy ATTN: DD

Defense Intelligence Agency
ATTN: DC-7D, W. Wittig
ATTN: DB-4C, E. O'Farrell
ATTN: HQ-TR, J. Stewart
ATTN: DB, A. Wise
ATTN: DT-5
ATTN: DT-1BZ, R. Morton
ATTN: DT-1B

Defense Nuclear Agency
ATTN: DDST
ATTN: STVL
3 cy ATTN: RAAE
4 cy ATTN: TITL

Field Command,
Defense Nuclear Agency
ATTN: FCPR

Interservice Nuclear Weapons School
ATTN: TTV

Joint Chiefs of Staff
ATTN: J-3, WMMCCS Evaluation Office

Joint Strat. Tgt. Planning Staff
ATTN: JPST, G. Goetz
ATTN: JLTW-2

Livermore Division, Field Command, DNA
Lawrence Livermore Laboratory
ATTN: FCPRL

National Security Agency
Department of Defense
ATTN: R52, J. Skillman
ATTN: B3, F. Leonard
ATTN: W32, O. Bartlett

Under Secretary of Defense for Rsch. & Engrg.
ATTN: Strategic & Space Systems (OS)

DEPARTMENT OF DEFENSE (Continued)

WMMCCS System Engineering Org.
ATTN: R. Crawford

DEPARTMENT OF THE ARMY

ERADCOM Technical Support Activity
Department of the Army
ATTN: DELET-ER, H. Bomke

Harry Diamond Laboratories
Department of the Army
ATTN: DELHD-N-NP

U.S. Army Foreign Science & Tech. Center
ATTN: DRXST-SD

U.S. Army Nuclear & Chemical Agency
ATTN: Library

DEPARTMENT OF THE NAVY

Naval Electronic Systems Command
ATTN: NAVELEX 3101, T. Hughes
ATTN: PME 117
ATTN: Code 5011
ATTN: PME 117-T

Naval Intelligence Support Center
ATTN: NISC-50

Naval Ocean Systems Center
ATTN: Code 8151, C. Baggett
3 cy ATTN: Code 5324, W. Moler

Naval Research Laboratory
ATTN: Code 7580
ATTN: Code 7555
ATTN: Code 7550, J. Davis
ATTN: Code 7500, Hg. Comm. Dir., B. Wald
ATTN: Code 6701, J. Brown

Naval Surface Weapons Center
ATTN: Code F31

Naval Surface Weapons Center
Dahlgren Laboratory
ATTN: Code F-14, R. Butler

Office of Naval Research
ATTN: Code 420
ATTN: Code 421

Office of the Chief of Naval Operations
ATTN: Op-604
ATTN: Op-941

Strategic Systems Project Office
Department of the Navy
ATTN: NSSP-2722, F. Wimberly
ATTN: NSP-2141

DEPARTMENT OF THE AIR FORCE

Air Force Technical Applications Center
ATTN: TF

Air Force Weapons Laboratory
ATTN: DYC, J. Barry
ATTN: SUL
ATTN: DYC, J. Kamm

DEPARTMENT OF THE AIR FORCE (Continued)

Deputy Chief of Staff
Research, Development, & Acq.
Department of the Air Force
ATTN: AFRDQ

Deputy Chief of Staff
Program and Analyses
Department of the Air Force
ATTN: PACSC, R. Paul

Electronic Systems Division, AFSC
ATTN: XRW, J. Deas
ATTN: YSEA
ATTN: PH, J. Whelan

Foreign Technology Division, AFSC
ATTN: TQTD, B. Ballard
ATTN: NISI, Library

Rome Air Development Center, AFSC
ATTN: Documents Library/TSLD

Rome Air Development Center, AFSC
ATTN: FEP

Strategic Air Command/XPFS
Department of the Air Force
ATTN: NRT
ATTN: DCX, Chief Scientist

OTHER GOVERNMENT AGENCIES

Central Intelligence Agency
ATTN: RD/SI, Rm. 5G48, Hq. Bldg.
for OSI/PSTD

Department of Commerce
National Bureau of Standards
ATTN: Sec. Officer for R. Moore

Institute for Telecommunications Sciences
National Telecommunications & Info. Admin.
ATTN: L. Berry
ATTN: A. Jean
ATTN: W. Utlaut
ATTN: D. Crombie

National Oceanic & Atmospheric Admin.
Environmental Research Laboratories
Department of Commerce
ATTN: Aeronomy Lab., G. Reid
ATTN: R. Grubb

DEPARTMENT OF DEFENSE CONTRACTORS

Analytical Systems Engineering Corp.
ATTN: Radio Sciences

Berkeley Research Associates, Inc.
ATTN: J. Workman

Boeing Co.
ATTN: G. Keister

University of California at San Diego
ATTN: H. Booker

Computer Sciences Corp.
ATTN: H. Blank

DEPARTMENT OF DEFENSE CONTRACTORS (Continued)

Cornell University
Department of Electrical Engineering
ATTN: D. Farley, Jr.

Electrospace Systems, Inc.
ATTN: H. Logston

Ford Aerospace & Communications Corp.
ATTN: J. Mattingley

General Electric Company-TEMPO
Center for Advanced Studies
ATTN: W. Knapp
ATTN: DASIAC

General Research Corp.
Santa Barbara Division
ATTN: J. Ise, Jr.
ATTN: J. Garbarino

Geophysical Institute
University of Alaska
ATTN: N. Brown
ATTN: T. Davis
ATTN: Technical Library

GTE Sylvania, Inc.
Electronics Systems Group-Eastern Div.
ATTN: M. Cross

Institute for Defense Analyses
ATTN: J. Aein

International Tel. & Telegraph Corp.
ATTN: Technical Library

JAYCOR
ATTN: S. Goldman

Johns Hopkins University
Applied Physics Lab.
ATTN: T. Potemra
ATTN: Document Librarian

Kaman Sciences Corp.
ATTN: T. Meagher

Lawrence Livermore Laboratory
University of California
ATTN: Doc. Con. for Technical Information
Dept. Library
ATTN: Doc. Con. for L-46, F. Seward

M.I.T. Lincoln Lab.
ATTN: D. Towle

Mission Research Corp.
ATTN: D. Sowle

Mitre Corp.
ATTN: C. Callahan
ATTN: G. Harding

Mitre Corp.
ATTN: W. Foster
ATTN: M. Horrocks
ATTN: W. Hall

DEPARTMENT OF DEFENSE CONTRACTORS (Continued)

Pacific-Sierra Research Corp.
ATTN: E. Field, Jr.

Pennsylvania State University
Ionosphere Research Lab.
ATTN: Ionospheric Research Lab.

R & D Associates
ATTN: R. Lelevier
ATTN: B. Gabbard
ATTN: C. Greifinger
ATTN: P. Greifinger

Rand Corp.
ATTN: C. Crain

DEPARTMENT OF DEFENSE CONTRACTORS (Continued)

Sandia Laboratories
Livermore Laboratory
ATTN: Doc. Con. for T. Cook
ATTN: Doc. Con. for B. Murphey

SRI International
ATTN: G. Carpenter
ATTN: G. Price
ATTN: W. Chesnut

79